

**Simulation Modeling of an Enhanced Low-Emission
Swirl-Cascade Burner**

SEMI-ANNUAL TECHNICAL PROGRESS REPORT

10/01/2003 through 3/31/2004

Dr. Ala Qubbaj, Mechanical Engineering Department

April 2004

DE-FG2602NT41682

**University of Texas pan American
1201 West University Drive
Edinburg, Texas 78539-2999**

DISCLAIMER NOTICE

This report was prepared as an account of work sponsored by an agency of the United States Government. Neither the United States Government nor any agency thereof, or any of their employees, makes any warranty, express or implied, or assumes any legal liability or responsibility of the accuracy, completeness, or usefulness of any information, apparatus, product, or process disclosed, or represents that its use would not infringe privately owned rights. Reference herein to any specific commercial product, process, or service by trade name, trademark, manufacturer, or otherwise does not necessarily constitute or imply its endorsement, recommendation, or favoring by the United States Government or any agency thereof. The views and opinions of authors expressed herein do not necessarily state or reflect those of the United States Government or any agency thereof.

ABSTRACT

Based on the physical and computational models outlined in the previous technical progress reports, Natural gas jet diffusion flames in baseline, cascade, swirl, and swirl-cascade burners were numerically modeled. The thermal, composition, and flow (velocity) fields were simulated. The temperature, CO₂ and O₂ concentrations, as well as the axial and radial velocity profiles were computed and analyzed. The numerical results showed that swirl and cascade burners have a more efficient fuel/air mixing, a shorter flame, and a lower NO_x emission levels, compared to the baseline case. The results also revealed that the optimal configurations of the cascaded and swirling flames have not produced an improved performance when combined together in a “swirl-cascade burner”.

TABLE OF CONTENTS

- I.** Title Page
- II.** Disclaimer Notice
- III.** Abstract
- IV.** Table of Contents
 - A.** Physical Model (Problem Geometry)
 - B.** Computational Model (Numerical Analysis)
 - C.** Results and Discussion
 - D.** Conclusions (Pending)
 - E.** References

A. PHYSICAL MODEL

The physical model and problem geometry were outlined in the preceding reports and are shown in Figure 1.

B. COMPUTATIONAL MODEL

The computational model and numerical Analysis were described in the preceding reports.

C. RESULTS AND DISCUSSION

Figure 2 shows the radial temperature profiles for baseline, cascaded, air-swirling, and swirling-cascaded flames in the near burner region, which corresponds to an axial location of $x/d=4.63$. This near burner region is of primary interest in this study since this is the area where most of the mixing and reactions take place. From the temperature profiles, the following observations can be made: (i) the off-axis peak exists in all cases, however, its radial location moves further inward in the cases of swirl and cascade and outward in the swirl-cascade; (ii) the peak temperature of the air-swirling and cascaded flames drop by 8% and 11%, respectively, from its baseline value, whereas that of the swirl-cascade increases by 8%; (iii) the swirl and cascade profiles are shifted inward towards the fuel-rich side of the flame, whereas the swirl-cascade one is shifted outward; (iv) the air-swirling and cascaded flames have significantly lower temperatures in the fuel-lean side of the flame, compared to the baseline case. However, it has higher valley temperatures in the fuel-rich side. The opposite trend is seen for the swirl-cascade.

The observed shift of the temperature profiles towards the fuel-rich side of the flame, in both the swirl and cascade cases, is a result of the air-swirling and venturi-cascade effects, respectively. The former produces a recirculation zone that sustains the entrainment process of the air stream into the fuel stream (Qubbaj et al.¹), Whereas, the latter ejects the co-flow air stream into the core of the combustion zone by the effect of the venturi. Both effects lead to a rapid homogenization and better mixing rates of air with the unburned fuel of the mixture, and the consequent shift of the stoichiometric contour towards the center of the flame. This leaning process has two different effects on the fuel-lean and fuel-rich sides of the flame; the temperature of the latter increases while that of the former decreases. The valley temperature increase in the fuel-rich side of the swirling and cascaded flames is a

result of higher oxygen availability, which pushes the mixture towards stoichiometry. On the other hand, the temperature decrease in the lean side is due to the excess air, which drives the mixture far away from stoichiometry. The higher peak temperature and outward shift of the swirl-cascade profiles indicate a poor mixing rates of air and fuel, and thereby counteracting the air-swirling and venturi effects seen earlier. The higher temperature would also suggest higher levels of NO_x.

Figure 3 depicts the radial concentration profiles of CO₂ at the same conditions pertaining to the earlier temperature profiles. The existence of off-axis peaks, their radial locations, the shift of the profiles, the CO₂ concentrations in the fuel rich and fuel-lean sides, all follow the temperature profiles and similar explanations apply. This is reasonable, since CO₂ is a direct combustion product, which depends primarily on temperature and stoichiometry of the flame.

Figure 4 shows the O₂ radial concentration profiles for the baseline, air-swirling, cascaded, and swirling-cascaded flames in the near-burner region. From these profiles the following can be observed: (i) the O₂ concentration starts with a zero value at the central axis and starts to build up in the radial outward direction until it attains its atmospheric value (~21%) near the outside boundary of the flame; (ii) O₂ concentration in the both air-swirling and cascaded flames build up faster and consequently attain the ambient value earlier than in the baseline and swirl-cascade cases; (iii) O₂ profiles in the air-swirling and cascaded flames are shifted inward, whereas that of the swirl-cascade is shifted outward. This observation is similar to that seen earlier for temperature and CO₂ profiles.

The zero O₂ concentration observed in the fuel-rich region is consistent with the absence of CO₂ values observed earlier in the same region. The faster build-up rates in the air-swirling and cascaded flames, compared to the baseline flame, is a clear indication of the higher rates of mixing with air provided by the air-swirling and venturi effects, respectively. This increase of O₂ is the direct cause of the temperature drop observed earlier. On the other hand, the lower build-up rate in the swirl-cascade case depicts poor mixing rates, thereby diminishing the swirling and venturi effects. The inward/outward shifts of the profiles have been noticed for the earlier temperature and CO₂ profiles too, and therefore, the same aforementioned explanation applies.

Figure 5 shows the radial profiles of the axial velocity component (U) for the baseline, cascaded, air-swirling, and swirl-cascaded flames in the near burner region. These profiles reveal that both air-swirling and cascaded flames have a lower centerline velocity and a wider profile than the baseline flame. The opposite trends are seen for the swirling-cascaded flame. The lower centerline velocity in the air-swirling and cascaded cases suggests a shorter flame produced by the swirl and venturi effects, respectively. However, when combined in the swirling-cascaded flame, the higher centerline velocity implies a longer flame.

In general, for a circular jet, the centerline velocity decreases and the jet becomes wider as the jet grows downstream due to the viscous shear and more air entrainment. Therefore, the lower centerline velocity and wider profiles observed for the air-swirling and cascaded flames, compared to the baseline case, are indications of the rapid and faster growth of the gas jet flame. However, this interpenetration process is due not to shear but rather to the air-swirling and venturi-cascade effects, respectively. The former effect induces a recirculation zone that sustains the entrainment process of the outer air stream into the inner fuel stream, whereas, the latter inducts more of the co-flow air stream into the combustion zone. Both effects present the capability of an efficient mixing between the streams in the regions near the fuel outlet, therefore leading to a rapid homogenization of the combustible mixture and a shortening of the flame. The higher O_2 concentration and lower axial centerline velocity, observed in Figs. 4 and 5 for the swirl and cascade cases, compared to the baseline case, substantiate the last verdict for a shorter flame. However, the opposite trends predicted in the swirl-cascade case supports the earlier argument of a longer flame.

The shorter flame length and the consequent shorter residence time (assuming constant flame velocity), combined with the predicted lower temperatures in Fig. 2, are strong indicatives of Low NO_x emission levels in the swirl and cascade cases. On the other hand, the opposite trends in the swirl-cascade case constitute a strong indication for a higher level of NO_x .

Figure 6 presents the transverse profiles of the radial velocity component (V) at the same conditions. The general trend for the baseline profile is that the radial velocity is zero at the centerline, then it increases to attain a peak value in the fuel-rich region, beyond which it starts decreasing until it reaches a minimum (negative) value close to the stoichiometric

contour, then it starts increasing again in the fuel-lean side of the flame to attain an asymptotic value near the flame edge. The positive velocities predicted close to centerline imply an outward velocity direction due to jet momentum. On the other hand, the negative velocities noticed farther from the centerline indicate an inward velocity direction. The swirl and cascade profiles reveal well-pronounced zones characterized by negative values of the velocity caused by the adverse pressure gradient induced by the intense swirl and venturi effects, respectively. Such a zone is less pronounced in the swirl-cascade case. Therefore, a dramatic increase in the inward radial velocities compared to the outward velocities is predicted for both swirl and cascade, compared to the baseline and swirl-cascade cases. The more negative radial velocities with the swirl and cascade cases indicate clearly the generation of an additional inward flow (towards the centerline of the jet) by the effects of the swirl and venturis, respectively, thereby leading to the higher rates of mixing and its consequent impact on the combustion process. However, such effects are diminished for the swirl-cascade case.

The last verdict appears to be surprising, since an enhanced performance was initially expected by combining the optimal performance of both swirl and cascade burners in what thought to be “an enhanced swirl-cascade burner”. Nevertheless, the numerical results showed that the optimal configurations of the cascaded and swirling flames would not necessarily produce an improved performance when combined together in a “swirl-cascade burner”. The location of the recirculation zone with respect to the venturi must have played an important role. In other words, the swirling and venturi-cascading (at such conditions) have hindered each other’s influence. The non-linearity and complexity of the system accounts for such a result, and therefore, all possible combinations, i.e. swirl numbers (SN) versus venturi diameter ratios (D/d), need to be considered.

D. CONCLUSION (pending)

The analysis of the above results is still underway; the conclusions will be made soon.

E. REFERENCES

None

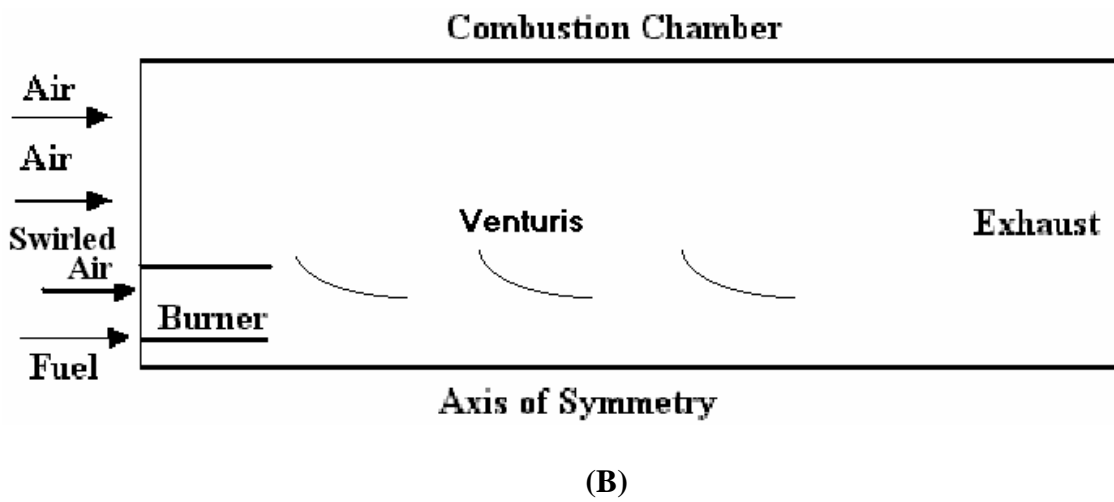
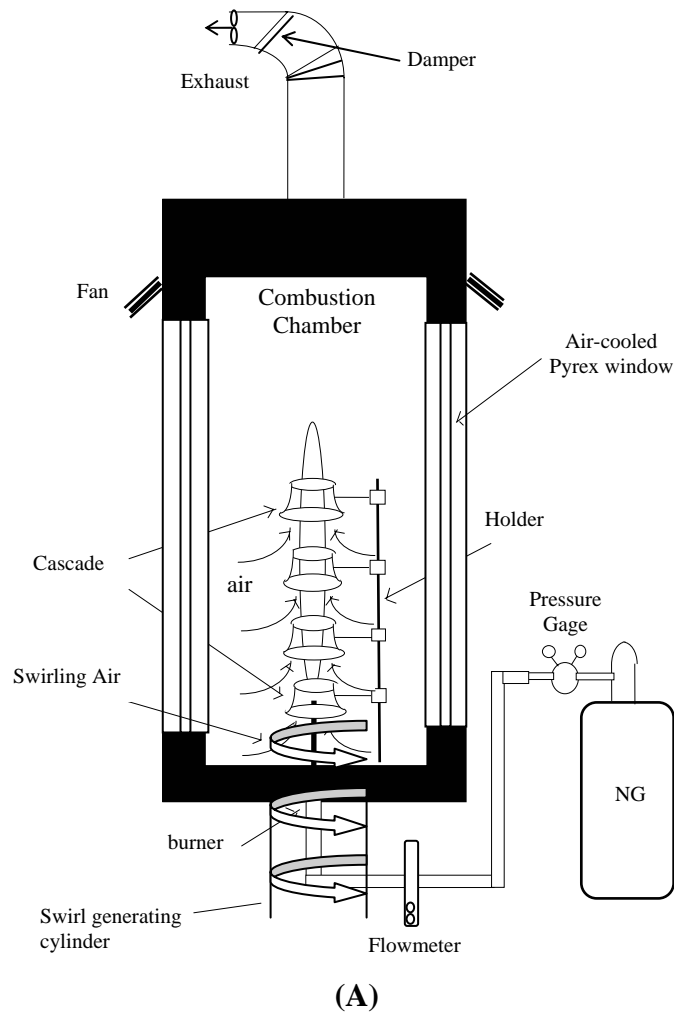


Figure1: (a) Actual physical model (b) Simplified Problem geometry

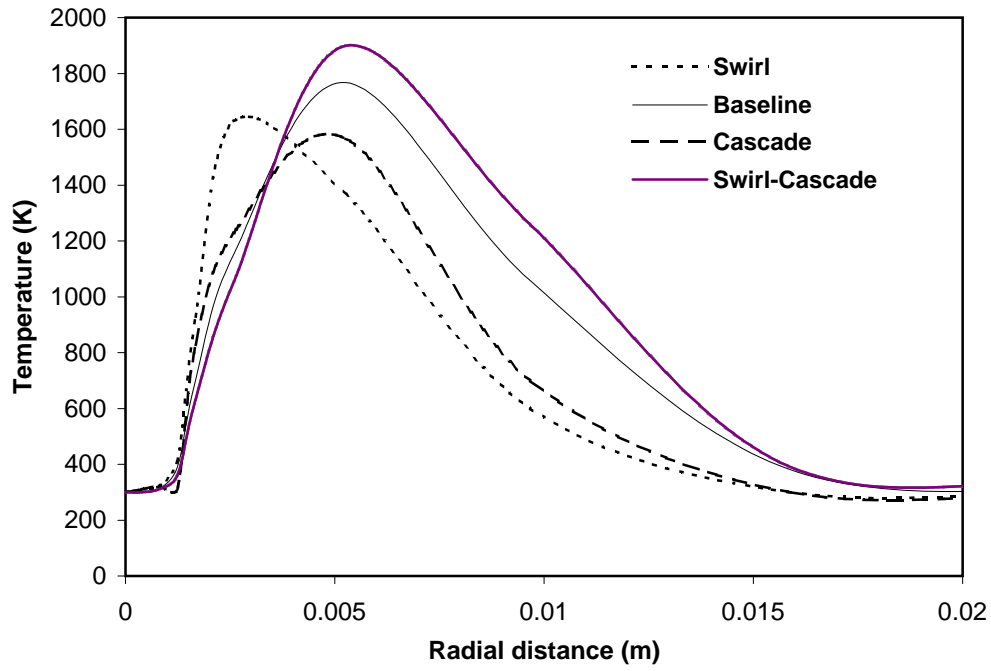


Fig. 2: Temperature Radial Profiles

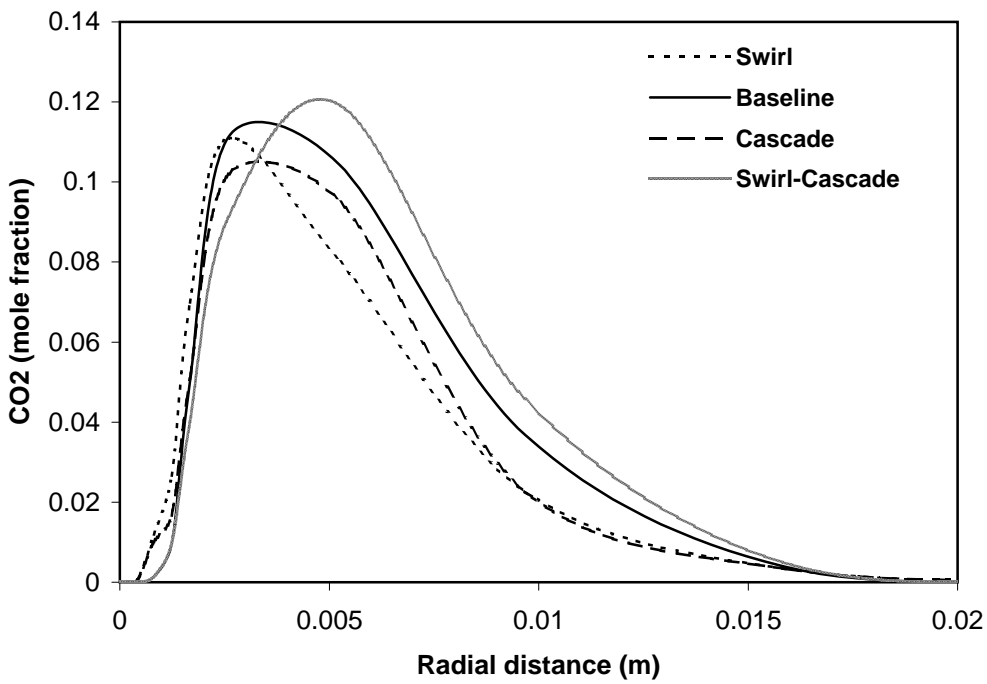


Fig. 3: Carbon Dioxide Radial Profiles

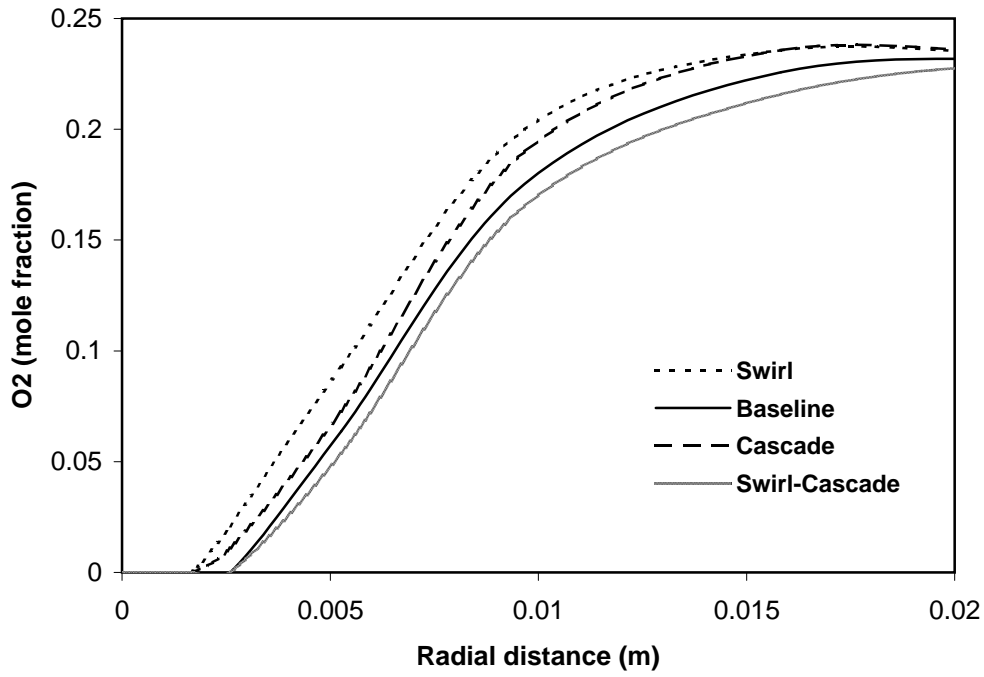


Fig. 4: Radial Oxygen Profiles

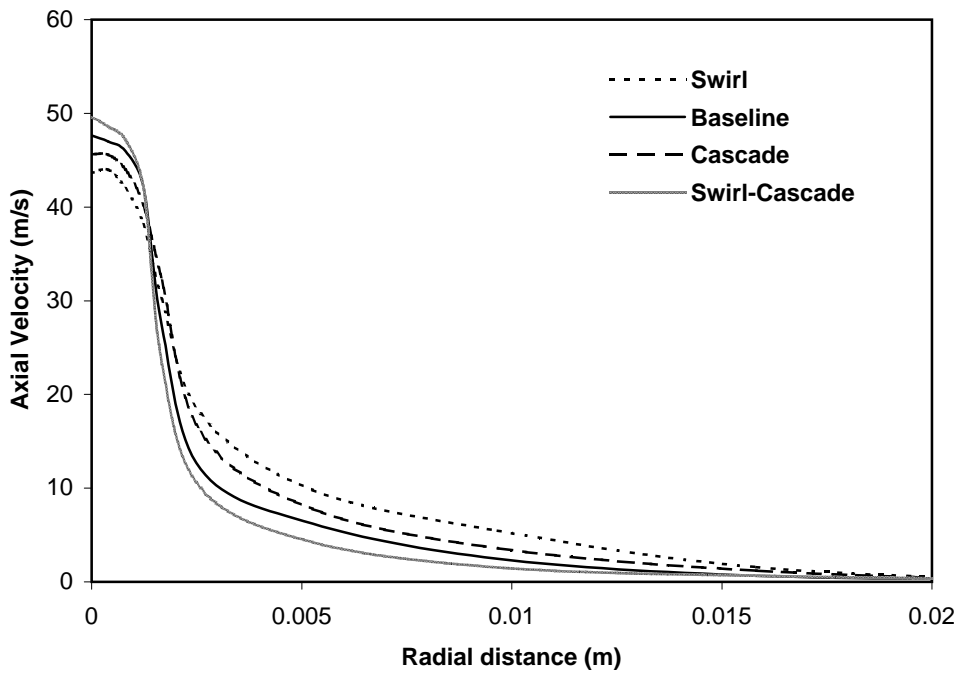


Fig. 5: Radial Profiles of Axial Velocity Component (U)

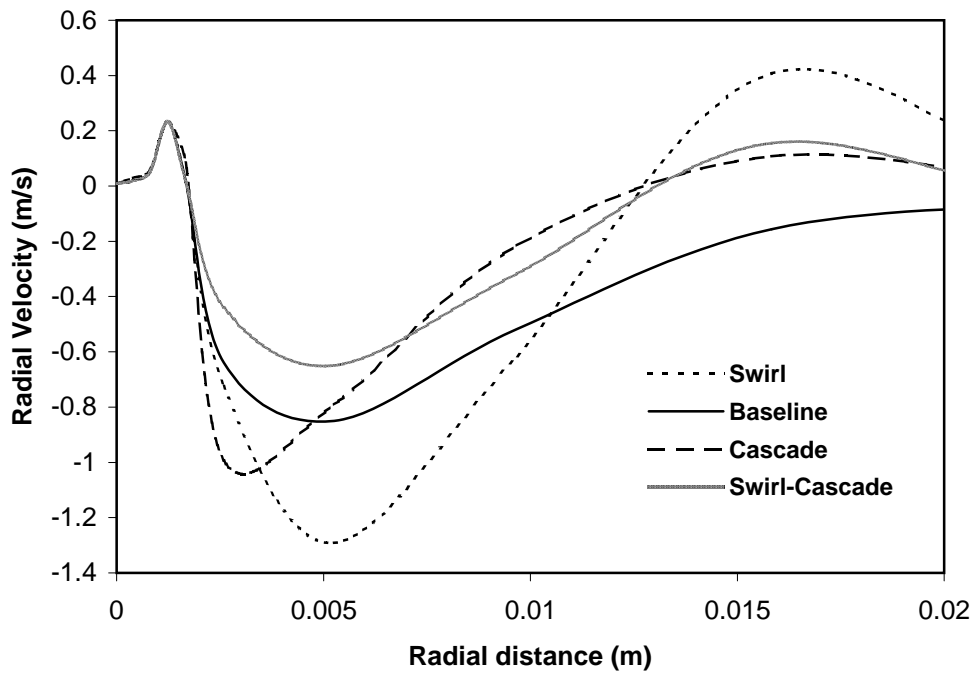


Fig. 6: Radial Profiles of Radial Velocity Component (V)